# Symmetry-based approach to electron-phonon interactions in graphene

J. L. Mañes
*Departamento de Física de la Materia Condensada, Universidad del País Vasco, Apartado 644, E-48080 Bilbao, Spain*
(Received 8 March 2007; revised manuscript received 13 June 2007; published 30 July 2007)

We use the symmetries of monolayer graphene to write a set of constraints that must be satisfied by any electron-phonon interaction Hamiltonian. The explicit solution as a series expansion in the momenta gives the most general, model-independent couplings between electrons and long-wavelength acoustic and optical phonons. As an application, the possibility of describing elastic strains in terms of effective electromagnetic fields is considered in detail, with an emphasis on group-theory conditions and the role of time-reversal symmetry.

DOI: 10.1103/PhysRevB.76.045430 PACS number(s): 63.20.Kr, 63.22.+m, 71.15.Rf

## I. INTRODUCTION

Symmetry plays an ubiquitous role in solid state physics, where invariance of the system under symmetry transformations imposes strong constraints on the form of Hamiltonians and other physical observables.[1,2] In computations of phonon spectra, the choice of convenient symmetry-adapted coordinates simplifies the diagonalization of the dynamical matrix.[3] Instead of a $3N\times 3N$ matrix, where $N$ is the number of atoms in the unit cell, we end up with a collection of smaller matrices, one per inequivalent irreducible representation (IR), with a dimension equal to the multiplicity of that representation in the "mechanical" representation. Similar simplifications take place in the computation of electronic bands.

An important *caveat* is that the symmetry which is effective in simplifying the problem is not the whole space group of the crystal but the little group[1] that preserves the wave vector of the electrons or phonons.[4] Thus, symmetry-based methods are really powerful around points and lines of high symmetry in the Brillouin zone. Since electron-phonon interactions involve generic wave vectors with trivial little groups, it would seem that symmetry considerations cannot be very helpful in that case. Indeed, many computations of electron-phonon interactions are based on the use of specific models (electron-ion interactions,[5,6] modulated hoppings,[7–9] phonon-modulated electron-electron interactions,[10] etc.), and little or no use is made of the symmetries of the system.

On the other hand, long-wavelength phonons play a crucial role in many physical processes of interest, such as transport phenomena, where electron-phonon interactions are essential.[5,6] The elements of the dynamical matrix for long-wavelength phonons (acoustic and optical) can be expanded as a power series in the phonon wave vector $q$, and this expansion is strongly constrained by the little group of the $\Gamma$ point, which of course coincides with the space group of the crystal. Unfortunately, low-energy electrons lie near the Fermi surface, where typical points lack any symmetry.

Graphene[11,12] is a remarkable exception in this regard. Instead of an ordinary Fermi surface, undoped monolayer graphene has two isolated, high symmetry Fermi points. Thus, as long as we restrict ourselves to long-wavelength phonons and low-energy electrons, which are necessarily close to the Fermi points, the interaction Hamiltonian will be strongly constrained by symmetry. In fact, in Sec. IV, we will be able to write the most general interaction Hamiltonian as an explicit series expansion around the $\Gamma$ point (for phonon wave vectors) and the Fermi points (for electron wave vectors).

One possible application of the Hamiltonian obtained here is to many-body computations,[6,13,14] where analytic expressions are often preferred over numerically defined functions. In the usual approach, a concrete model, such as the one based on phonon-modulated nearest neighbor hoppings, is used to compute an interaction Hamiltonian which later is expanded to the required order in the momenta.[10,13,15] Alternatively, one can take the interaction Hamiltonian given in Sec. IV as a power expansion and keep terms up to the order desired. Obviously, less effort is involved by this method, and one is sure that all possible couplings have been included, whereas a particular model may miss some of them. The obvious drawback is that symmetry arguments by themselves do not give a clue as to the values of the parameters. Another very different application of the electron-phonon Hamiltonian is presented in Sec. V, where we investigate a description of elastic strains in terms of effective electromagnetic fields.[16]

This paper is organized as follows. In Sec. II, we review the symmetries of monolayer graphene and the transformation properties of electrons and phonons. Section III presents a study of the dynamical matrix including the form of the long-wavelength normal modes. The phonon-electron interactions are computed in Sec. IV, and the results are used in Sec. V to study the possibility of interpreting trilinear electron-phonon couplings in terms of effective scalar and vector potentials. The conclusions are presented in Sec. VI.

## II. SYMMETRIES

We begin this section with a description of electrons and phonons in monolayer graphene, including the choice of the symmetry-adapted modes to be used in the rest of this paper. We then proceed to study their transformation properties.

### A. Electrons and phonons

Monolayer graphene consists of a honeycomb lattice. The corresponding hexagonal Bravais lattice is generated by $\vec{t}_1=(a\sqrt{3},0)$ and $\vec{t}_2=(a\sqrt{3}/2,3a/2)$, where $a$ is the distance be-

 

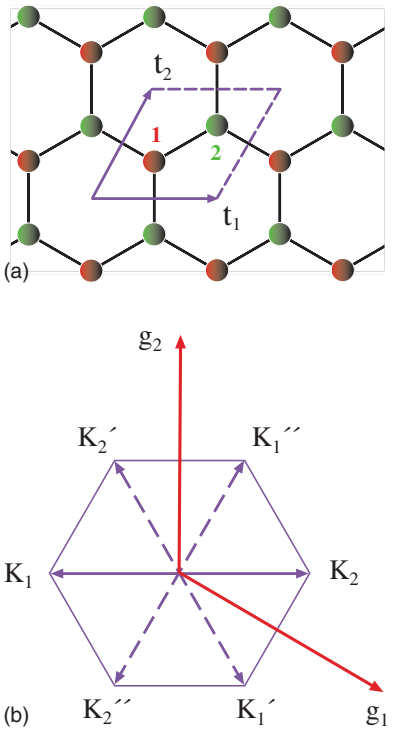


FIG. 1. (Color online) Top: Direct lattice and unit cell for monolayer graphene. Bottom: First Brillouin zone and Fermi points. The vectors $\vec{K}_1', \vec{K}_1''$ $(\vec{K}_2', \vec{K}_2'')$ are equivalent to $\vec{K}_1$ $(\vec{K}_2)$.

tween nearest neighbors (see Fig. 1). The unit cell contains two atoms, with positions given by $\vec{r}_1=\vec{t}_1/3+\vec{t}_2/3$ and $\vec{r}_2=2\vec{r}_1$. The reciprocal lattice is generated by $\vec{g}_1=(2\pi/\sqrt{3}a, -2\pi/3a)$ and $\vec{g}_2=(0,4\pi/3a)$, with $\vec{t}_i\cdot\vec{g}_j=2\pi\delta_{ij}$. Corresponding to the two atoms in the unit cell, we may define two Bloch wave functions,

$$\Phi_i(\vec{K}) = \sum_{\vec{t}} e^{i\vec{K}\cdot(\vec{r}_i+\vec{t})}\Phi(\vec{r}-\vec{r}_i-\vec{t}), \quad i=1,2, \tag{1}$$

where the sum runs over all the points in the direct lattice, i.e., $\vec{t}=n_1\vec{t}_1+n_2\vec{t}_2$ and $\Phi(\vec{r})$ is a real $\pi$-type atomic orbital. As is well known, a simple tight-binding computation[17,18] yields a spectrum with two Fermi points located at $\vec{K}_1=-2\vec{g}_1/3-\vec{g}_2/3$ and $\vec{K}_2=-\vec{K}_1$. Near the two Fermi points, the Hamiltonian can be linearized and one finds

$$H(\vec{K}_1+\vec{k}) \sim \frac{3}{2}at\begin{pmatrix} 0 & k^* \\ k & 0 \end{pmatrix}, \quad k \equiv k_x + ik_y, \tag{2}$$

where $t$ is the hopping integral, and $H(-\vec{K}_1+\vec{k})=H^*(\vec{K}_1-\vec{k})$. Thus, the low-energy electronic excitations behave like massless Dirac fermions[19,20] with relativistic spectrum $E=\pm v_F|k|$. Henceforth, we assume that our units are such that $v_F=3at/2=1$.

In this paper, we want to consider the interaction between electrons near the Fermi points $\{\vec{K}_1,-\vec{K}_1\}$ and phonons $Q(\vec{q})$ for small values of $q$. Due to invariance under reflection by the horizontal plane $\sigma_h$, only in-plane modes can couple linearly to electrons. Thus, for most of this paper, we consider only in-plane modes, which are specified by giving the horizontal displacements $u(\vec{t})=(x_1,y_1,x_2,y_2)$ of the two atoms in the unit cell with origin at the lattice point $\vec{t}$ (see, however, sec. V, where quadratic couplings of out-of-plane acoustic modes are considered in the long-wavelength limit).

TABLE I. In-plane symmetry-adapted modes for monolayer graphene. Here, $e_i(q)=\frac{1}{2}e^{i\vec{q}\cdot\vec{r}_i}$, where $\{\vec{r}_i\}$ are the equilibrium positions of the two atoms in the unit cell.

| | $u_1$ | $u_2$ | $u_1'$ | $u_2'$ |
|---|---|---|---|---|
| $x_1$ | $e_1(q)$ | $e_1(q)$ | $e_1(q)$ | $e_1(q)$ |
| $y_1$ | $ie_1(q)$ | $-ie_1(q)$ | $ie_1(q)$ | $-ie_1(q)$ |
| $x_2$ | $e_2(q)$ | $e_2(q)$ | $-e_2(q)$ | $-e_2(q)$ |
| $y_2$ | $ie_2(q)$ | $-ie_2(q)$ | $-ie_2(q)$ | $ie_2(q)$ |

We can choose a basis of symmetry-adapted modes with particularly simple transformation properties by noting that, under a point group transformation, a mode undergoes two changes: the vectors describing atomic displacements are rotated or reflected according to the vector representation, and there is a permutation among equivalent atoms. This last effect may give rise to annoying phases in the transformation matrices, which can be avoided by incorporating appropriate phases into the definitions of the modes. The use of circularly rather than linearly polarized modes simplifies the effect of rotations.

Our choice of in-plane modes is given in Table I. In the long-wavelength limit $qa \ll 1$, the phases vanish $e_i(q) \to 1$ and the unprimed (primed) modes become circularly polarized acoustic (optical) normal modes, respectively (see Sec. III for details). This basis is used to expand general in-plane displacements $u(\vec{t})=(x_1,y_1,x_2,y_2)$ as follows:

$$u(\vec{t}) = \sum_q \left[ \sum_{i=1}^{2} Q_i(\vec{q})u_i(\vec{q}) + \sum_{i=1}^{2} Q_i'(\vec{q})u_i'(\vec{q}) \right] e^{i\vec{q}\cdot\vec{t}}. \tag{3}$$

### B. Transformation properties

The space group of monolayer graphene is symmorphic, with point group $D_{6h}$ (see Ref. 2 for conventions and notation). $D_{6h}$ is generated by $\{C_6^+,\sigma_{v1},\sigma_h\}$, where $C_6^+$ is a counterclockwise rotation by $\pi/3$ around the $z$ axis, $\sigma_{v1}$ is a reflection by the $xz$ plane, and $\sigma_h$ is a reflection by the horizontal $xy$ plane that contains the graphene layer. However, given the planar structure of the system and as long as we are restricted to in-plane modes, we will consider instead the normal subgroup $C_{6v}$, generated by $\{C_6^+,\sigma_{v1}\}$. The little point group of $\vec{K}_1$ is $\hat{G}_{\vec{K}_1}=C_{3v}$, generated by $\{C_3^+,\sigma_{v1}\}$. The star of $\vec{K}_1$ consists of the two Fermi points $\{\vec{K}_1,-\vec{K}_1\}$. Since the binary rotation $C_2$ around the $z$ axis transforms $\vec{K}_1$ into $-\vec{K}_1$, it is convenient to use $\{C_3^+,\sigma_{v1},C_2\}$ as a (redundant) set of generators for $C_{6v}$.

The action of the generators of $C_{6v}$ on the modes in Table I is given in Appendix A. As a result of a symmetry operation $g$, a displacement with wave vector $q$ is transformed into

a new displacement with wave vector $gq$ and coordinates $\{gQ_i, qQ_i'\}$. Defining $Q \equiv \{Q_1, Q_2\}$ and $Q' \equiv \{Q_1', Q_2'\}$, the transformation properties can be written as

$$gQ(gq) = T(g)Q(q), \quad gQ'(gq) = T'(g)Q'(q), \tag{4}$$

where $T'(C_2) = -T(C_2) = \mathbf{1}$ is the unit matrix, and

$$T(\sigma_{v1}) = -T'(\sigma_{v1}) = \sigma_x = \begin{pmatrix} 0 & 1 \\ 1 & 0 \end{pmatrix},$$

$$T(C_3^+) = T'(C_3^+) = \Omega \equiv \begin{pmatrix} \omega^* & 0 \\ 0 & \omega \end{pmatrix}, \tag{5}$$

with $\omega \equiv \exp(2\pi i/3)$.

Another important symmetry is the time reversal, which acts by complex conjugation. According to Table I,

$$\mathcal{T}: u_1^*(q) = u_2(-q), \quad u_2^*(q) = u_1(-q), \tag{6}$$

with identical action on $u_i'$. Then, reality of a general displacement [Eq. (3)] implies

$$Q^*(q) = \sigma_x Q(-q), \quad Q'^*(q) = \sigma_x Q'(-q). \tag{7}$$

We now turn our attention to the electrons. Since low-energy electronic excitations are located near the two Fermi points, it is convenient to change variables, $\vec{K} = \pm\vec{K}_1 + \vec{k}$. Correspondingly, we define Bloch functions $\Phi_{i\pm}(k)$ in the neighborhoods of the Fermi points,

$$\Phi_{i\pm}(k) \equiv \Phi_i(\pm\vec{K}_1 + \vec{k}). \tag{8}$$

The action of the generators of $C_{6v}$ on the wave functions is given in Appendix A. As long as we do not consider the spin, time reversal acts simply by complex conjugation. According to Eq. (1), $\Phi_i^*(\vec{K}) = \Phi_i(-\vec{K})$. Thus, time reversal exchanges the two Fermi points and we have

$$\mathcal{T}: \Phi_{i+}(k) \to \Phi_{i+}^*(k) = \Phi_{i-}(-k),$$

$$\Phi_{i-}(k) \to \Phi_{i-}^*(k) = \Phi_{i+}(-k). \tag{9}$$

As both time reversal $\mathcal{T}$ and the binary rotation $C_2$ around the $z$ axis reverse the sign of the wave vector, the combined symmetry $\mathcal{T}C_2$ preserves the Fermi points. Note, however, that the two atoms are exchanged,

$$\mathcal{T}C_2: \Phi_{1+}(k) \leftrightarrow \Phi_{2+}(k), \quad \Phi_{2-}(k) \leftrightarrow \Phi_{1-}(k). \tag{10}$$

This combined symmetry plays an important role in the computation of electron-phonon interactions in Sec. IV and is behind the topological stability of Fermi points in mono- and multilayer graphene.[22]

## III. DYNAMICAL MATRIX

The modes in Table I have simple transformation properties, but they do not correspond to normal modes with well defined frequencies. In general, these must be obtained by numerical diagonalization of the dynamical matrix.[23–25] However, in the long-wavelength regime, one can easily obtain useful analytical results by exploiting the symmetries of the system.

The symmetries constrain the form of the dynamical matrix $V(q)$ defined by

$$E_p = \frac{m}{2}\sum_q \mathbf{Q}^\dagger(q)V(q)\mathbf{Q}(q), \tag{11}$$

where $\mathbf{Q} = \{Q, Q'\}$ stands for the four symmetry-adapted coordinates in Eq. (3), $m$ is the mass of the carbon atom, and the sum is over the first Brillouin zone. The Hermitian matrix $V$ can be decomposed into $2\times 2$ blocks,

$$V(q) = \begin{pmatrix} D & M \\ M^\dagger & D' \end{pmatrix}, \tag{12}$$

associated with the unprimed and primed modes. Then, invariance under a spatial symmetry [Eq. (4)] gives

$$\mathbf{T}(g)V(q)\mathbf{T}^\dagger(g) = V(gq), \tag{13}$$

with

$$\mathbf{T}(g) = \begin{pmatrix} T(g) & 0 \\ 0 & T'(g) \end{pmatrix}, \tag{14}$$

whereas invariance under time reversal [Eq. (7)] implies

$$\mathcal{T}V^*(q)\mathcal{T} = V(-q), \quad \mathcal{T} = \begin{pmatrix} \sigma_x & 0 \\ 0 & \sigma_x \end{pmatrix}. \tag{15}$$

Neglecting initially the acoustic-optical mixing due to $M$, we can obtain an approximation to acoustic frequencies and modes by solving a $2\times 2$ eigenvalue problem,

$$D(q)u(q) = \omega^2(q)u(q), \tag{16}$$

where $u(q)$ is a linear combination of the two unprimed modes given in Table I. As shown in Appendix B, the symmetry constrains the form of the Hermitian matrix $D$ to

$$D(q) = \begin{pmatrix} a(q) & b(q) \\ b^*(q) & a(q) \end{pmatrix}, \tag{17}$$

where $a(q)$ and $b(q)$ are even functions of $q$ that satisfy

$$a(\omega q) = a(q), \quad b(\omega q) = \omega b(q),$$

$$a(q^*) = a(q), \quad b(q^*) = b^*(q). \tag{18}$$

The eigenvalue problem is solved by

$$\omega_\pm^2(q) = a(q) \pm |b(q)|, \tag{19}$$

with normal modes given by

$$u_\pm(q) = \frac{1}{\sqrt{2}}\left[u_1(q)\frac{b(q)}{|b(q)|} \pm u_2(q)\right]. \tag{20}$$

In the absence of acoustic-optical interactions, this is the most general acoustic spectrum compatible with the symmetries of the system. For small $q$, this solution admits a simple geometric interpretation. Expanding $a(q)$ and $b(q)$,

$$a(q) = a_2|q|^2 + a_4|q|^4 + O(q^6),$$

$$b(q) = b_2 q^{*2} + b_4 |q|^2 q^{*2} + \tilde{b}_4 q^4 + O(q^6), \tag{21}$$

where all the constants are real, and keeping only the quadratic terms yields

$$\omega_{L,T}^2(q) = (a_2 \pm b_2)|q|^2, \tag{22}$$

where the + (−) sign goes with $\omega_L^2$ ($\omega_T^2$). The normal modes are

$$u_L(q) = \frac{1}{\sqrt{2}|q|}[q^* u_1(q) + q u_2(q)],$$

$$u_T(q) = -\frac{i}{\sqrt{2}|q|}[q^* u_1(q) - q u_2(q)]. \tag{23}$$

These represent longitudinal acoustic (LA) and transverse acoustic (TA) modes, respectively. To see this, note that for $qa \ll 1$, we have

$$u_L(q) \simeq \frac{1}{\sqrt{2}} \begin{pmatrix} \cos\theta \\ \sin\theta \\ \cos\theta \\ \sin\theta \end{pmatrix}, \quad u_T(q) \simeq \frac{1}{\sqrt{2}} \begin{pmatrix} -\sin\theta \\ \cos\theta \\ -\sin\theta \\ \cos\theta \end{pmatrix}, \tag{24}$$

where $q = |q| e^{i\theta}$, i.e., $\theta = \tan^{-1}(q_y/q_x)$. In the long-wavelength limit, the normal modes are completely independent of the coefficients in the dynamical matrix.

We can easily go beyond the quadratic approximation in $q$ valid in the long-wavelength limit by keeping more terms in the expansions [Eq. (21)]. Keeping just the first anisotropic contributions gives

$$\omega_{L,T}^2(q) = (a_2 \pm b_2)|q|^2 + |q|^4(a_4 \pm b_4 \pm \tilde{b}_4 \cos 6\theta) + O(q^6). \tag{25}$$

One can use the perturbation theory to compute the leading corrections $u_{L,T} \to u_{L,T} + \delta u_{L,T}$ to the normal modes. Taking as perturbation the fourth order corrections to $D$,

$$\delta D = \begin{pmatrix} a_4|q|^4 & b_4|q|^2 q^{*2} + \tilde{b}_4 q^4 \\ b_4|q|^2 q^2 + \tilde{b}_4 q^{*4} & a_4|q|^4 \end{pmatrix}, \tag{26}$$

yields

$$\delta u_L \simeq \frac{u_T^\dagger \delta D u_L}{\omega_L^2 - \omega_T^2} u_T \simeq -\frac{\tilde{b}_4}{2b_2}|q|^2 \sin 6\theta u_T,$$

$$\delta u_T \simeq \frac{u_L^\dagger \delta D u_T}{\omega_T^2 - \omega_L^2} u_L \simeq \frac{\tilde{b}_4}{2b_2}|q|^2 \sin 6\theta u_L. \tag{27}$$

Thus, beyond the long-wavelength approximation, the normal modes are not purely transverse or longitudinal, and Eq. (27) shows that this longitudinal-transverse (LT) mixing is an $O(q^2)$ anisotropic effect.

The solution to the eigenvalue problem for the optical modes is very similar. The elements of the matrix $D'(q)$ satisfy the same constraints [Eq. (18)], but the diagonal elements need not vanish for $q=0$. Keeping just the quadratic contributions

$$D'(q) = \begin{pmatrix} \omega_0^2 + a_2'|q|^2 & b_2' q^{*2} \\ b_2' q^2 & \omega_0^2 + a_2'|q|^2 \end{pmatrix}, \tag{28}$$

we find that the optical normal modes $u_L'$ and $u_T'$ are given by Eq. (23) in terms of the primed modes $u_i'$, with normal frequencies

$$\omega_{L,T}'^2(q) = \omega_0^2 + (a_2' \pm b_2')|q|^2. \tag{29}$$

Similarly, LT mixing for optical modes is still given by Eq. (27) if one uses primed constants.

We can also study acoustic-optical (AO) mixing, which is induced by the matrix $M$. For example, keeping only the leading contributions to $M$ (see the Appendix B for details),

$$M(q) \simeq e_1 \begin{pmatrix} 0 & q \\ -q^* & 0 \end{pmatrix}, \tag{30}$$

and using perturbation theory yields the following corrections to the LA and TA modes:

$$\delta u_L \simeq \frac{i e_1}{\omega_0^2}|q|(\sin 3\theta u_L' + \cos 3\theta u_T'),$$

$$\delta u_T \simeq \frac{i e_1}{\omega_0^2}|q|(\cos 3\theta u_L' - \sin 3\theta u_T'). \tag{31}$$

Thus, AO mixing is an $O(q/\omega_0^2)$ anisotropic effect. Exchanging primed and unprimed modes in Eq. (31) gives the corrections to the optical modes. This mixing induces a common shift in the frequencies of the acoustic modes,

$$\delta\omega_L^2 = \delta\omega_T^2 \simeq -\frac{e_1^2}{\omega_0^2}|q|^2, \tag{32}$$

while the opposite shift is induced in the optical frequencies.

## IV. ELECTRON-PHONON COUPLINGS

In this section, we use a similar strategy to obtain the most general interaction Hamiltonian compatible with the symmetries of the system. We consider an electron-phonon interaction Hamiltonian of the form

$$H_{e\text{-}ph} = \sum_{ij,k,q} H_{ij}(k,q,\mathbf{Q}) c_{i+}^\dagger(k+q/2) c_{j+}(k-q/2) + \sum_{ij,k,q} H_{-ij}(k,q,\mathbf{Q}) c_{i-}^\dagger(k+q/2) c_{j-}(k-q/2), \tag{33}$$

where $c_{i\pm}(k)$ annihilates an electron in the state $\Phi_{i\pm}(k)$ given by Eq. (8) and $\mathbf{Q} = \{Q, Q'\}$ stands for the four symmetry-adapted coordinates in Eq. (3). The somewhat unusual parametrization of initial and final electron momenta $(k \mp q/2)$ simplifies the form of the constraints. The matrix element is given by

$$H_{ij}(k,q,\mathbf{Q}) = \langle \Phi_{i+}(k+q/2)|V_{ei}|\Phi_{j+}(k-q/2)\rangle, \tag{34}$$

where $V_{ei}$ is the electron-ion potential. Since the two Fermi points are related both by time reversal and by $C_2$, either symmetry can be used to obtain the form of the Hamiltonian near $\vec{K}_2 = -\vec{K}_1$, giving

$$H_-(k,q,\mathbf{Q}) = H^*(-k,-q,\mathbf{Q}), \tag{35}$$

where

$$H_{-ij}(k,q,\mathbf{Q}) \equiv \langle \Phi_{i-}(k+q/2)|V_{ei}|\Phi_{j-}(k-q/2)\rangle. \tag{36}$$

Thus, we can restrict ourselves to the Hamiltonian in the vicinity of $\vec{K}_1$.

On the other hand, the combined symmetry $C_2\mathcal{T}$ [Eq. (10)] leaves the two Fermi points invariant and can be used to impose a constraint on $H(k,q,C_2\mathbf{Q})$,

$$H(k,q,C_2\mathbf{Q}) = \sigma_x H^*(k,q,\mathbf{Q})\sigma_x, \tag{37}$$

which is solved by

$$H(k,q,\mathbf{Q}) = \begin{pmatrix} \alpha(k,q,\mathbf{Q}) & \beta(k,q,\mathbf{Q}) \\ \beta^*(k,q,C_2\mathbf{Q}) & \alpha^*(k,q,C_2\mathbf{Q}) \end{pmatrix}, \tag{38}$$

where $\alpha$ and $\beta$ are arbitrary complex functions. Note that the hermiticity of the Hamiltonian does *not* imply reality for $\alpha$. The point is that the matrix $H(k,q,C_2\mathbf{Q})$ connects initial and final states with different momenta, and instead we have

$$\begin{aligned} H_{ij}(k,q,\mathbf{Q}) &= \langle \Phi_{i+}(k+q/2)|V_{ei}|\Phi_{j+}(k-q/2)\rangle \\ &= \langle \Phi_{j+}(k-q/2)|V_{ei}|\Phi_{i+}(k+q/2)\rangle^* \\ &= H^*_{ji}(k,-q,\mathbf{Q}) \end{aligned} \tag{39}$$

which implies

$$\alpha(k,-q,\mathbf{Q}) = \alpha^*(k,q,\mathbf{Q}),$$

$$\beta(k,-q,\mathbf{Q}) = \beta(k,q,C_2\mathbf{Q}). \tag{40}$$

Finally, we must impose invariance under the little point group $C_{3v}$,

$$T^\dagger(g)H(k,q,\mathbf{Q})T(g) = H(gk,gq,g\mathbf{Q}), \tag{41}$$

where $T(g)$ is given by Eq. (5). The Hamiltonian [Eq. (38)] together with the constraints [Eqs. (40) and (41)] contains the most general interactions beween electrons and in-plane phonon compatible space group and time-reversal symmetries. These constraints are analyzed in detail in Appendix C, where the general solution for the interaction Hamiltonian is found in the form

$$H(k,q,\mathbf{Q}) = H(k,q,Q) + H'(k,q,Q'), \tag{42}$$

with

$$\begin{aligned} H(k,q,Q) &= i\begin{pmatrix} f(k,q)Q_1(q) - f(k,-q)^*Q_2(q) & g_1(k,q)Q_1(q) + g_2(k,q)Q_2(q) \\ g_2(k,q)^*Q_1(q) + g_1(k,q)^*Q_2(q) & -f(k,-q)Q_1(q) + f(k,q)^*Q_2(q) \end{pmatrix}, \\ H'(k,q,Q') &= i\begin{pmatrix} f'(k,q)Q'_1(q) - f'(k,-q)^*Q'_2(q) & g'_1(k,q)Q'_1(q) + g'_2(k,q)Q'_2(q) \\ -g'_2(k,q)^*Q'_1(q) - g'_1(k,q)^*Q'_2(q) & f'(k,-q)Q'_1(q) - f'(k,q)^*Q'_2(q) \end{pmatrix}. \end{aligned} \tag{43}$$

The functions entering the Hamiltonian must satisfy some simple conditions. In particular, the functions $f$, $f'$, $g_2$, and $g'_2$ must satisfy identical constraints, which we write only for $f$,

$$f(\omega k,\omega q) = \omega f(k,q), \quad f(k^*,q^*) = f(k,q)^*, \tag{44}$$

whereas the conditions on $g_1$ and $g'_1$ are

$$g_1(\omega k,\omega q) = g_1(k,q), \quad g_1(k^*,q^*) = g_1(k,q)^*. \tag{45}$$

Besides, we must have

$$g_i(k,-q) = -g_i(k,q), \quad g'_i(k,-q) = g'_i(k,q). \tag{46}$$

Since $\omega^3=1$, one immediately sees that any combination of monomials of the form

$$k^n k^{*n'} q^m q^{*m'} \tag{47}$$

with real coefficients and $n-n'+m-m'=1 \bmod 3$ will satisfy Eq. (44). Imposing instead $n-n'+m-m'=0 \bmod 3$, we will get solutions to Eq. (45). Finally, conditions (46) are satisfied by taking $m+m'$ odd (even) for $g_i$ ($g'_i$).

Equation (43) together with the comments around Eq. (47) can be used to expand the interaction Hamiltonian to any order in $q$ and $k$, giving all possible in-plane phonon-electron couplings compatible with the symmetries of monolayer graphene, and is the main result in this paper. For the rest of this section, we will study the long-wavelength limit and some leading corrections.

Consider first the coupling to acoustic phonons. Taking into account that the interaction should vanish for $q\to 0$, we can immediately write the leading contributions to the functions $f, g_1, g_2$,

$$f(k,q) \approx \sqrt{2}\alpha_1 q, \quad g_1(k,q) \approx 0, \quad g_2(k,q) \approx \sqrt{2}\beta_1 q, \tag{48}$$

where $\alpha_1$ and $\beta_1$ are real constants and the $\sqrt{2}$ has been introduced for later convenience. This gives

$$\begin{aligned} &H(k,q,Q) \\ &\approx i\sqrt{2}\begin{pmatrix} \alpha_1(qQ_1(q) + q^*Q_2(q)) & \beta_1 qQ_2(q) \\ \beta_1 q^*Q_1(q) & \alpha_1(qQ_1(q) + q^*Q_2(q)) \end{pmatrix}. \end{aligned} \tag{49}$$

For some physical applications, it may be more convenient to express the Hamiltonian as a function of normal

rather than symmetry-adapted coordinates. As we know from the previous section, the longitudinal and transverse modes in Eq. (23) are a good approximation to the actual normal modes in the long-wavelength limit. Using

$$Q_1 = \frac{q^*}{\sqrt{2}|q|}(Q_L - iQ_T), \quad Q_2 = \frac{q}{\sqrt{2}|q|}(Q_L + iQ_T), \quad (50)$$

the interaction Hamiltonian takes the following form:

$$H(k,q,Q) \approx i|q| \begin{pmatrix} 2\alpha_1 Q_L & \beta_1 e^{2i\theta}(Q_L + iQ_T) \\ \beta_1 e^{-2i\theta}(Q_L - iQ_T) & 2\alpha_1 Q_L \end{pmatrix}, \quad (51)$$

where $\theta = \tan^{-1}(q_y/q_x)$ is the phase of $q = |q|e^{i\theta}$. This shows that TA phonons do not couple diagonally to electrons in the long-wavelength limit, which is parametrized by the two real coulplings $\alpha_1$ and $\beta_1$. This form of the Hamiltonian can be used to write Eq. (33) in terms of phonon creation and annihilation operators,[6] with $Q_{L,T}(q) = (2\omega_{L,T})^{-1/2}[a_{L,T}(q) + a^\dagger_{L,T}(-q)]$.

Note that even if one is primarily interested in acoustic phonons, because of the acoustic-optical mixing discussed in the last section, one may have to consider the couplings of electrons to optical modes as well. Since the couplings to optical modes do not have to vanish as $q \to 0$, the leading contributions to the Hamiltonian are independent of $q$. These are found to be

$$H(k,q,Q') \approx i\sqrt{2}\beta_1' \begin{pmatrix} 0 & Q_1' \\ -Q_2' & 0 \end{pmatrix} = i\beta_1' \begin{pmatrix} 0 & e^{-i\theta}(Q_L' - iQ_T') \\ -e^{i\theta}(Q_L' + iQ_T') & 0 \end{pmatrix}, \quad (52)$$

where $\beta_1'$ is a real constant.

We can easily include higher powers of the momenta. For instance, for acoustic phonons, the contribution of order $O(q^2)$ is parametrized by a single real constant $\alpha_2$ and is purely diagonal and proportional to the Pauli matrix $\sigma_z$,

$$\Delta H(k,q,Q) = \alpha_2 |q|^2 (Q_L \sin 3\theta + Q_T \cos 3\theta)\sigma_z. \quad (53)$$

This is qualitatively different from the leading contribution [Eq. (51)] due to the anisotropy in the strength of the electron-phonon couplings and the diagonal contribution of TA phonons. The contribution of order $O(q)$ for optical phonons is proportional to the unit matrix

$$\Delta H'(k,q,Q') = i\alpha_2' |q| Q_L' \mathbf{1}, \quad (54)$$

and there is also an $O(k)$ term given by

$$\Delta H'(k,q,Q') = \alpha_3' |k| [Q_L' \sin(\varphi - \theta) + Q_T' \cos(\varphi - \theta)]\mathbf{1}, \quad (55)$$

where $\varphi = \tan^{-1}(k_y/k_x)$. The contributions of order $O(qk)$ are more complicated and depend on five real constants. Note that as we move away from the $\Gamma$ point, the LA and TA modes given by Eq. (23) are no longer a good approximation to the normal modes of the system, and one has to take into account the LT and AO mixings considered in the previous section.

Electron-phonon interactions can be rewritten in terms of electrons and holes. The eigenstates for the electron Hamiltonian [Eq. (2)] are given by

$$\Phi_\pm(k) = \frac{1}{\sqrt{2}}[e^{-i\varphi/2}\Phi_1(k) \pm e^{i\varphi/2}\Phi_2(k)], \quad (56)$$

and this can be used to obtain the matrix elements between electron eigenstates, with $H_{++}$ and $H_{--}$ ($H_{+-}$ and $H_{-+}$) corresponding to intraband (interband) transitions. Of course, if we decide to include higher powers of $k$ in the electron-phonon Hamiltonian, for consistency we must also go beyond the low-energy Dirac hamiltonian [Eq. (2)]. The corrections to the electronic Hamiltonian are fixed by symmetry. Note, in particular, that the electronic Hamiltonian can be considered as the **Q**-independent part of Eq. (34). Then, Eq. (38) reduces to

$$H(k) = \begin{pmatrix} \alpha_0(k) & \beta_0(k) \\ \beta_0^*(k) & \alpha_0^*(k) \end{pmatrix}, \quad (57)$$

where hermiticity (40) implies that $\alpha_0$ is real. The little group constraints [Eq. (C1)] simplify to

$$C_3^+ : \alpha_0(\omega k) = \alpha_0(k), \quad \beta_0(\omega k) = \omega^* \beta_0(k),$$

$$\sigma_{v1} : \alpha_0(k^*) = \alpha_0(k)^*, \quad \beta_0(k^*) = \beta_0(k)^*, \quad (58)$$

which can be easily solved to any order in $k$. Taking the chemical potential at half filling as the origin of energies and $v_F = 1$, the first few terms are

$$\alpha_0(k) = \alpha_{0,2}|k|^2 + \alpha_{0,3}(k^3 + k^{*3}) + \cdots,$$

$$\beta_0(k) = k^* + \beta_{0,2}k^2 + \beta_{0,3}|k|^2 k^* + \cdots, \quad (59)$$

where all the constants are real. The eigenstates are still given by Eq. (56) if one replaces the phase of $k$ by the phase of $\beta_0^*(k)$.

## V. ELASTIC STRAINS AS EFFECTIVE ELECTROMAGNETIC FIELDS

Here, we show that the couplings of long-wavelength phonons to electrons have some similarities—and differences—with those of the scalar and vector potentials for the electromagnetic field. We show, in particular, that both in-plane and out-of-plane strains can mimic some of the effects of electric and magnetic fields.

The minimal coupling prescription $k_i \to k_i + A_i$ on Eq. (2) gives

$$H(k) = \begin{pmatrix} \Phi & k^* + A^* \\ k + A & \Phi \end{pmatrix}, \quad H_-(k) = \begin{pmatrix} \Phi & -k - A \\ -k^* - A^* & \Phi \end{pmatrix}, \quad (60)$$

where $A = A_x + iA_y$ is the vector potential in complex notation and $\Phi$ is the scalar (electric) potential. For the purposes of

this section, it is convenient to change from the circularly polarized modes of Table I to linear modes $u_x$, $u_y$,

$$u_1 = \frac{1}{\sqrt{2}}(u_x + iu_y), \quad u_2 = \frac{1}{\sqrt{2}}(u_x - iu_y),$$

$$Q_1 = \frac{1}{\sqrt{2}}(Q_x - iQ_y), \quad Q_2 = \frac{1}{\sqrt{2}}(Q_x + iQ_y). \tag{61}$$

Then, the acoustic Hamiltonian [Eq. (49)] can be rewritten by using

$$i\sqrt{2}(qQ_1 + q^*Q_2) = 2i(q_xQ_x + q_yQ_y),$$

$$i\sqrt{2}qQ_2 = 2i(q_xQ_x - q_yQ_y) - 2(q_xQ_y + q_yQ_x),$$

$$i\sqrt{2}q^*Q_1 = 2i(q_xQ_x - q_yQ_y) + 2(q_xQ_y + q_yQ_x). \tag{62}$$

This agrees with the Hamiltonian given in Ref. 15, where the off-diagonal elements (second and third lines) were obtained by expanding a phonon-modulated hopping, while the magnitude of the diagonal element, known as "deformation potential," was estimated in a nearly free electron model. Our derivation shows that both diagonal and off-diagonal terms are uniquely determined by symmetry.

Taking Fourier transforms with $iq_i \to \partial_i$ and comparing with Eq. (60) finally yields

$$\Phi(K_1) = \Phi(K_2) = 2\alpha_1(\partial_xQ_x + \partial_yQ_y),$$

$$A_x(K_1) = -A_x(K_2) = 2\beta_1(\partial_xQ_x - \partial_yQ_y),$$

$$A_y(K_1) = -A_y(K_2) = -2\beta_1(\partial_xQ_y + \partial_yQ_x), \tag{63}$$

where we have used Eq. (35) to obtain the electron-phonon Hamiltonian around $\vec{K}_2$. These effective fields can be written in terms of elastic strains with the usual definitions

$$u_{xx} = \partial_xQ_x, \quad u_{yy} = \partial_yQ_y, \quad 2u_{xy} = \partial_xQ_y + \partial_yQ_x. \tag{64}$$

Thus, we have the remarkable result that, around each Fermi point, static strains can mimic the effects of external electric and magnetic fields.

We also see that the couplings of electrons near the two Fermi points are identical for the scalar potential but differ by a sign for the vector potential. Thus, for static strains, they will experience the same "electrostatic" field but opposite "magnetic" fields given by

$$\begin{aligned} B_z(K_1) &= -B_z(K_2) \\ &= \partial_xA_y(K_1) - \partial_yA_x(K_1) \\ &= -2\beta_1[(\partial_x^2 - \partial_y^2)Q_y + 2\partial_x\partial_yQ_x] \\ &= -2\beta_1[2\partial_xu_{xy} + \partial_y(u_{xx} - u_{yy})]. \end{aligned} \tag{65}$$

We now address the following question: Is the (partial) identification between elastic strains and effective electromagnetic fields peculiar to graphene alone or can we expect to find it in other systems? The first observation is straightforward: The minimal coupling prescription $\vec{k} \to \vec{k} + \vec{A}$ gives rise to the required type of interactions for the vector potential only if the electron system satisfies the Dirac equation. An ordinary nonrelativistic equation would produce terms of the type $\vec{k}\cdot\vec{A}$, where $\vec{k}$ is the electron momentum, unlike the leading phonon couplings [Eq. (49)], which are $k$ independent.

However, even with Dirac points, further conditions have to be satisfied. The effective fields [Eq. (63)] associated with acoustic phonons are of the form $\partial_iQ_j$, where both $\partial_i$ and $Q_i$ belong to the vector representation $V$. The vector potential also belongs to $V$. In the continuum, $V \times V$ and $V$ have opposite parities, and $\partial_iQ_j$ and $A$ cannot transform equivalently. Thus, the possibility of describing elastic strains as effective fields is a lattice effect. More concretely, we need a lattice without inversion symmetry.

However, even on a lattice, this identification can be partial at best. The reason is that the vector potential is odd under time reversal, whereas phonons and their derivatives are even. Since time reversal takes $\vec{K}$ to $-\vec{K}$, as long as $-\vec{K}$ is not equivalent to $\vec{K}$, we can still hope for a partial identification valid around individual Fermi points. This will be possible only if the representations $V$ and $V \times V$ of the *little* group $G_{\vec{K}}$ have at least one irreducible representation in common, i.e., if $V^3$ contains the identity (or trivial) representation.

We now discuss how these conditions are met by monolayer graphene. The little group is $\hat{G}_{\vec{K}_1} = C_{3v}$ with a vector representation that decomposes according to[2]

$$V = A_1(z) + E(x,y). \tag{66}$$

For in-plane modes, only $E$ is relevant, and the use of elementary group-theory techniques[1,2] yields

$$\begin{aligned} E \times E = {} & A_1(\partial_xQ_x + \partial_yQ_y) + A_2(\partial_xQ_y - \partial_yQ_x) \\ & + E(\partial_yQ_y - \partial_xQ_x, \partial_xQ_y + \partial_yQ_x). \end{aligned} \tag{67}$$

Here, we recognize the left-hand side of Eq. (63) as the basis for the irreducible representations $A_1$ and $E$. However, the fact that the vector potential $(A_x, A_y)$ and certain components of the strain tensor transform equivalently under the little point group $C_{3v}$ is not sufficient to guarantee that elastic strains can mimic a magnetic field around each Fermi point, for they could still couple to the two atoms in the unit cell with different signs. By Eq. (10), the two atoms are exchaged under $C_2\mathcal{T}$. Now, the vector potential is odd under $C_2$ and $\mathcal{T}$, whereas the in-plane components of the elastic strain are even under both symmetries, and the two minus signs cancel each other. However, electrons at the two Fermi points see effective vector potentials which differ by the sign. On the other hand, the scalar potential $\Phi$ belongs to the trivial representation $A_1$ and is even under time reversal. As a consequence, the effective scalar potential takes the same sign on $\vec{K}_1$ and $\vec{K}_2 = -\vec{K}_1$.

This analysis can be extended to include the effects of so-called ripples or long-wavelength deformations perpendicular to the graphene sheet. Such ripples make the two-dimensional graphene sheet thermodynamically stable and have been recently observed in individually suspended sheets.[29] Although we have restricted ourselves to in-plane

modes, acoustic out-of-plane modes can easily be incorporated in the long-wavelength limit (see Sec. VI for the possibility of a more general analysis).

According to Eq. (66), a vertical displacement $Q_z$ belongs to the IR $A_1$ of $C_{3v}$. On the other hand, $Q_z$ is odd under reflection by the horizontal plane $\sigma_h$, whereas electronic wave function bilinears are necessarily even. This forces us to consider *quadratic* functions of $Q_z$. By translation invariance along the $z$ axis, only derivatives of $Q_z$ are acceptable, and we have to consider quadratic functions of $\partial_x Q_z$ and $\partial_y Q_z$. The bases for the IRs $A_1$ and $E$ are now given by

$$A_1[(\partial_x Q_z)^2 + (\partial_y Q_z)^2],$$

$$E[(\partial_y Q_z)^2 - (\partial_x Q_z)^2, 2\partial_x Q_z \partial_y Q_z]. \tag{68}$$

The discussion after Eq. (67) applies also in this case, implying that the couplings of electrons near the two Fermi points are identical for the scalar potential but differ by a sign for the vector potential. Thus, the associated effective fields are given by

$$\Phi(K_1) = \Phi(K_2) = \gamma[(\partial_x Q_z)^2 + (\partial_y Q_z)^2],$$

$$A_x(K_1) = -A_x(K_2) = \delta[(\partial_y Q_z)^2 - (\partial_x Q_z)^2],$$

$$A_y(K_1) = -A_y(K_2) = 2\delta \partial_x Q_z \partial_y Q_z, \tag{69}$$

where $\gamma$ and $\delta$ are real coupling constants.

We close this section by noting that frozen optical modes can also give rise to effective magnetic fields.[33] Indeed, the substitution of Eq. (61) into Eq. (52) gives

$$H(k,q,Q') = i\sqrt{2}\beta_1' \begin{pmatrix} 0 & Q_1' \\ -Q_2' & 0 \end{pmatrix} = \beta_1' \begin{pmatrix} 0 & Q_y' + iQ_x' \\ Q_y' - iQ_x' & 0 \end{pmatrix}. \tag{70}$$

Comparing with the minimally coupled Hamiltonians [Eq. (60)] yields the identifications

$$A_x'(K_1) = -A_x'(K_2) = \beta_1' Q_y',$$

$$A_y'(K_1) = -A_y'(K_2) = -\beta_1' Q_x', \tag{71}$$

and the magnetic fields

$$B_z'(K_1) = -B_z'(K_2) = -\beta_1'(\partial_x Q_x' + \partial_y Q_y'). \tag{72}$$

## VI. DISCUSSION

In this paper, we have exploited the fact that, for many physical processes of interest in monolayer graphene, the wave vectors of electrons and phonons lie near points of high symmetry in the Brillouin zone. Even though the little groups for nonvanishing $k$ and $q$ are generically trivial, the proximity to points of high symmetry impose strong constraints on the series expansions of observables around them. This is analogous to the situation in Landau's theory[1] of second order phase transitions, where the dependence on the order parameter of observables in the low symmetry phase is determined by the space group of the *high* symmetry phase. Here, $q$ and $k$ play the role of order parameters, "breaking" the symmetries of the $\Gamma$ and Fermi points, respectively. As a consequence, the method presented in this paper may be useful in other systems with Fermi points, such as multilayer graphene.[22,26–28] Semimetals with small electron and hole pockets around high symmetry points are also good candidates.

Note that, in spite of the fact that we use tight-binding Bloch functions as our starting point, our results are model independent. The reason is that only the symmetry properties of the wave functions are used, and the general electronic Hamiltonian [Eq. (57)] describes any doublet of states transforming according to the small representation $E$ of the little group.

The relatively involved constraints [Eqs. (40) and (41)] on the electron-phonon Hamiltonian are reduced to extremely simple conditions on the few functions which appear in the general solution [Eq. (43)] in Sec. IV—so simple, indeed, that they can be solved explicitly. In the process, the general functions $\alpha$ and $\beta$ are written as *linear* combinations of the symmetry-adapted coordinates. By dropping the linearity assumption, we could extend our approach to multiphonon processes. One can easily check that the constraints [Eqs. (40) and (41)] are still valid for nonlinear functions depending on several modes and momenta, with

$$\alpha(k,q,\mathbf{Q}) \to \alpha(k,\{q_l\},\{\mathbf{Q}_l(q_l)\}), \tag{73}$$

and other obvious replacements. Note that at the nonlinear level, out-of-plane modes have to be included for consistency, and the whole symmmetry $D_{6h}$ rather than $C_{6v}$ has to be used. The analysis becomes more involved and will be the object of future work.

Inspired by a mechanism first proposed in Ref. 30 for the case of dislocations in multivalley conductors, effective magnetic fields induced by elastic distorsions have been recently suggested as a way to explain the strong suppression of weak localization in graphene.[31,32] This differs from our results in Sec. V in that they consider effective gauge fields which are *quadratic* in the out-of-plane modes. Our analysis in the previous section shows that in-plane modes give rise to efffective fields, which are linear in the strains. For physical applications of the treatment in Sec. V to dislocations and other deffects, see Ref. 33.

Our method can be easily extended to accomodate external fields. For instance, in the presence of an electric field along the $z$ axis, out-of-plane phonons will couple linearly to the electrons. This may be an externally applied electric field or the effect of a substrate which breaks the symmetry under reflections on the sample plane. The recently observed ripples in suspended graphene sheets[29] also break the reflection symmetry $\sigma_h$ and can play the role of a "background field," inducing new electron-phonon interactions.

## ACKNOWLEDGMENTS

It is a pleasure to thank F. Guinea for motivating this work and for very useful discussions and suggestions, particularly in reference to Sec. V. This work has been sup-

ported in part by the Spanish Science Ministry under Grant No. FPA2005-04823.

## APPENDIX A: TRANSFORMATIONS OF MODES AND WAVE FUNCTIONS

The action of the generators of $C_{6v}$ on the electron and phonon wave vectors is given by the vector representation. This is simpler in the complex notation

$$C_3^+ q = \omega q, \quad \sigma_{v1} q = q^*, \quad C_2 q = -q, \quad \omega \equiv e^{2\pi i/3}, \tag{A1}$$

where $q = q_x + iq_y$.

Careful inspection of Table I shows that the generator $C_3^+$ acts identically on primed and unprimed symmetry-adapted modes, namely,

$$C_3^+ : u_1(q) \to \omega^* u_1(\omega q), \quad u_2(q) \to \omega u_2(\omega q), \tag{A2}$$

where $\omega \equiv \exp(2\pi i/3)$. The actions of $\sigma_{v1}$ and $C_2$, however, are different for the two types of modes,

$$\sigma_{v1} : u_1(q) \to u_2(q^*), \quad u_2(q) \to u_1(q^*),$$

$$u_1'(q) \to -u_2'(q^*), \quad u_2'(q) \to -u_1'(q^*),$$

$$C_2 : u_i(q) \to -u_i(-q), u_i'(q) \to u_i'(-q). \tag{A3}$$

Correspondingly, the symmetry-adapted coordinates $Q_i$ and $Q_i'$ in Eq. (3) have transformation properties

$$gQ(gq) = T(g)Q(q), \quad gQ'(gq) = T'(g)Q'(q), \tag{A4}$$

where $T'(C_2) = -T(C_2) = \mathbf{1}$ is the unit matrix, and

$$T(\sigma_{v1}) = -T'(\sigma_{v1}) = \sigma_x = \begin{pmatrix} 0 & 1 \\ 1 & 0 \end{pmatrix},$$

$$T(C_3^+) = T'(C_3^+) = \Omega \equiv \begin{pmatrix} \omega^* & 0 \\ 0 & \omega \end{pmatrix}. \tag{A5}$$

Note that at the $\Gamma$ point, the unprimed (primed) modes transform according to the two-dimensional representation $E_1$ ($E_2$) of $C_{6v}$.

The action of the generators of the little group $C_{3v}$ on the electronic wave functions is given by

$$C_3^+ : \Phi_{1+}(k) \to \omega \Phi_{1+}(\omega k), \quad \Phi_{2+}(k) \to \omega^* \Phi_{2+}(\omega k),$$

$$\Phi_{1-}(k) \to \omega^* \Phi_{1-}(\omega k), \quad \Phi_{2-}(k) \to \omega \Phi_{2-}(\omega k),$$

$$\sigma_{v1} : \Phi_{1+}(k) \leftrightarrow \Phi_{2+}(k^*), \quad \Phi_{1-}(k) \leftrightarrow \Phi_{2-}(k^*). \tag{A6}$$

The binary axis $C_2$ connects the two Fermi points

$$C_2 : \Phi_{1+}(k) \leftrightarrow \Phi_{2-}(-k), \quad \Phi_{2+}(k) \leftrightarrow \Phi_{1-}(-k). \tag{A7}$$

Equations (A6) and (A7) imply that, at the Fermi points ($k = 0$), the wave functions $\{\Phi_{i\pm}(0)\}$ form the basis for the four-dimensional IR $E$ of the space group,[21] with star $\{\vec{K}_1, -\vec{K}_1\}$.

## APPENDIX B: SYMMETRIES OF THE DYNAMICAL MATRIX

Since according to Eq. (13) invariance under the generators of $C_{3v}$ impose identical constraints on $D$ and $D'$, we write these only for $D$,

$$C_3^+ : D(\omega q) = \Omega D(q) \Omega^*, \quad \sigma_{v1} : D(q^*) = \sigma_x D(q) \sigma_x. \tag{B1}$$

The nondiagonal block $M$ satisfies the same constraint under $C_3^+$ but gets an additional minus sign under $\sigma_{v1}$,

$$\sigma_{v1} : M(q^*) = -\sigma_x M(q) \sigma_x. \tag{B2}$$

Invariance under $C_2$ implies that $D$ and $D'$ are even functions of $q$, whereas $M$ is odd,

$$C_2 : D(-q) = D(q), \quad D'(-q) = D'(q), \quad M(-q) = -M(q). \tag{B3}$$

Finally, time-reversal invariance [Eq. (7)] imposes the additional constraint

$$D(-q) = \sigma_x D^*(q) \sigma_x, \tag{B4}$$

which is also satisfied by $D'$ and $M$. Combining this equation with Eqs (B1)–(B3) gives

$$D(q^*) = D^*(q), \quad D'(q^*) = D'^*(q), \quad M(q^*) = M^*(q). \tag{B5}$$

These constraints are solved by

$$D(q) = \begin{pmatrix} a(q) & b(q) \\ b^*(q) & a(q) \end{pmatrix}, \tag{B6}$$

where $a(q)$ and $b(q)$ are even functions of $q$ that satisfy

$$a(\omega q) = a(q), \quad b(\omega q) = \omega b(q),$$

$$a(q^*) = a(q), \quad b(q^*) = b^*(q), \tag{B7}$$

with identical solution for $D'(q)$. For the off-diagonal block, the solution is

$$M(q) = \begin{pmatrix} d(q) & e(q) \\ -e(q^*) & -d(q^*) \end{pmatrix}, \tag{B8}$$

where $d(q)$ and $e(q)$ are odd functions of $q$ that satisfy the following constraints:

$$d(\omega q) = d(q), \quad e(\omega q) = \omega e(q),$$

$$d(q^*) = d^*(q), \quad e(q^*) = e^*(q). \tag{B9}$$

These imply the expansions

$$d(q) = d_3 q^3 + \tilde{d}_3 q^{*3} + O(q^5),$$

$$e(q) = e_1 q + e_3 |q|^2 q + O(q^5), \tag{B10}$$

where all the constants are real.

## APPENDIX C: LITTLE GROUP CONSTRAINTS ON THE ELECTRON-PHONON HAMILTONIAN

Substitution of Eq. (38) into Eq. (41) yields the following constraints on the complex functions $\alpha$ and $\beta$:

$$C_3^+:\alpha(\omega k,\omega q,C_3^+\mathbf{Q})=\alpha(k,q,\mathbf{Q}),$$

$$\beta(\omega k,\omega q,C_3^+\mathbf{Q})=\omega^*\beta(k,q,\mathbf{Q}),$$

$$\sigma_{v1}:\alpha(k^*,q^*,\sigma_{v1}\mathbf{Q})=\alpha^*(k,q,C_2\mathbf{Q}),$$

$$\beta(k^*,q^*,\sigma_{v1}\mathbf{Q})=\beta^*(k,q,C_2\mathbf{Q}), \tag{C1}$$

where the argument of $\mathbf{Q}$ is always the second one in the function, i.e., $\alpha(\omega k,\omega q,C_3^+\mathbf{Q})$ actually stands for $\alpha[\omega k,\omega q,C_3^+\mathbf{Q}(\omega q)]$. The general solution to the constraints can be found by writing

$$\alpha(k,q,\mathbf{Q})=\alpha(k,q,Q)+\alpha'(k,q,Q'),$$

$$\beta(k,q,\mathbf{Q})=\beta(k,q,Q)+\beta'(k,q,Q'), \tag{C2}$$

with

$$\alpha(k,q,Q)=i[f_1(k,q)Q_1(q)+f_2(k,q)Q_2(q)],$$

$$\beta(k,q,Q)=i[g_1(k,q)Q_1(q)+g_2(k,q)Q_2(q)], \tag{C3}$$

and equivalent expressions for $\alpha'$ and $\beta'$ in terms of primed variables. Then, substitution of $\alpha$ into hermiticity conditions (40) gives

$$f_2(k,q)=-f_1(k,-q)^*, \tag{C4}$$

which implies

$$\alpha(k,q,Q)=i[f(k,q)Q_1(q)-f^*(k,-q)Q_2(q)], \tag{C5}$$

with identical results for $\alpha'$. Imposing conditions (40) on $\beta$ and $\beta'$ gives

$$g_i(k,-q)=-g_i(k,q),\quad g_i'(k,-q)=g_i'(k,q). \tag{C6}$$

Substitution into the little group constraints [Eq. (C1)] shows that the functions $f$, $f'$, $g_2$, and $g_2'$ must satisfy identical conditions, which we write only for $f$,

$$f(\omega k,\omega q)=\omega f(k,q),\quad f(k^*,q^*)=f(k,q)^*, \tag{C7}$$

whereas the conditions on $g_1$ and $g_1'$ are

$$g_1(\omega k,\omega q)=g_1(k,q),\quad g_1(k^*,q^*)=g_1(k,q)^*. \tag{C8}$$

The general solution for the electron-phonon Hamiltonian is then given by Eqs. (42) and (43).


[1] G. Y. Lyubarskii, *The Application of Group Theory in Physics* (Pergamon, Oxford, 1960).
[2] C. J. Bradley and A. P. Cracknell, *The Mathematical Theory of Symmetry in Solids* (Clarendon, Oxford, 1972).
[3] A. A. Maradudin and S. H. Vosko, Rev. Mod. Phys. **40**, 1 (1968).
[4] Symmetry elements that do not belong to the little group can be used to relate observables at different points of the Brillouin zone, but they do not impose constraints on the form of observables at a particular point.
[5] J. M. Ziman, *Electrons and Phonons* (Oxford, New York, 1960).
[6] G. D. Mahan, *Many-Particle Physics*, 2nd ed. (Plenum, New York, 1990).
[7] S. Barisic, J. Labbe, and J. Friedel, Phys. Rev. Lett. **25**, 919 (1970).
[8] L. Pietronero, S. Strassler, H. R. Zeller, and M. J. Rice, Phys. Rev. B **22**, 904 (1980).
[9] R. A. Jishi, M. S. Dresselhaus, and G. Dresselhaus, Phys. Rev. B **48**, 11385 (1993).
[10] G. D. Mahan and L. M. Woods, Phys. Rev. B **60**, 5276 (1999).
[11] K. S. Novoselov, A. K. Geim, S. V. Morozov, D. Jiang, Y. Zhang, S. V. Dubonos, I. V. Gregorievna, and A. A. Firsov, Science **306**, 666 (2004).
[12] K. S. Novoselov, D. Jiang, T. Booth, V. Khotkevich, S. M. Morozov, and A. K. Geim, Proc. Natl. Acad. Sci. U.S.A. **102**, 10451 (2005).
[13] L. M. Woods and G. D. Mahan, Phys. Rev. B **61**, 10651 (2000).
[14] A. H. Castro Neto and F. Guinea, Phys. Rev. B **75**, 045404 (2007).
[15] H. Suzuura and T. Ando, Phys. Rev. B **65**, 235412 (2002).
[16] I am indebted to F. Guinea for suggesting this application and for bringing Ref. 32 to my attention.
[17] P. R. Wallace, Phys. Rev. **71**, 622 (1947).
[18] J. C. Slonczewski and P. R. Weiss, Phys. Rev. **109**, 272 (1948).
[19] J. González, F. Guinea, and M. A. H. Vozmediano, Phys. Rev. Lett. **69**, 172 (1992).
[20] J. González, F. Guinea, and M. A. H. Vozmediano, Nucl. Phys. B **406**, 771 (1993).
[21] As the space group is symmorphic, the IRs at the $K$ point can be labeled by those of the little point group $C_{3v}$, which are $A_1$, $A_2$, and $E$. Throughout this paper, we follow the notation and conventions of Ref. 2.
[22] J. L. Mañes, F. Guinea, and M. A. H. Vozmediano, Phys. Rev. B **75**, 155424 (2007).
[23] M. Maeda, Y. Kuramoto, and C. Horie, J. Phys. Soc. Jpn. **47**, 337 (1979).
[24] A. Sédéki, L. G. Caron, and C. Bourbonnais, Phys. Rev. B **62**, 6975 (2000).
[25] J. Maultzsch, S. Reich, C. Thomsen, H. Requardt, and P. Ordejón, Phys. Rev. Lett. **92**, 075501 (2004).
[26] J. Nilsson, A. H. Castro Neto, N. M. R. Peres, and F. Guinea, Phys. Rev. B **73**, 214418 (2006).
[27] J. Nilsson, A. H. Castro Neto, F. Guinea, and N. M. R. Peres, Phys. Rev. Lett. **97**, 266801 (2006).
[28] K. S. Novoselov, E. McCann, S. V. Morozov, V. I. Falko, M. I. Katsnelson, U. Zeitler, D. Jiang, F. Schedin, and A. K. Geim, Nat. Phys. **2**, 177 (2006).
[29] J. C. Meyer, A. K. Geim, M. I. Katsnelson, K. S. Novoselov, T. S. Booth, and S. Roth, Nature (London) (to be published).
[30] S. V. Iordanskii and A. E. Koshelev, JETP Lett. **41**, 575 (1985).
[31] A. F. Morpurgo and F. Guinea, Phys. Rev. Lett. **97**, 196804 (2006).
[32] S. V. Morozov, K. S. Novoselov, M. I. Katsnelson, F. Schedin, L. A. Ponomarenko, D. Jiang, and A. K. Geim, Phys. Rev. Lett. **97**, 016801 (2006).
[33] F. Guinea *et al.* (unpublished).